Shear Force Distribution in RC Slabs Subjected To Punching: Solid Nonlinear FE Analyses

SHEAR FORCE DISTRIBUTION IN RC SLABS SUBJECTED TO PUNCHING: SOLID NONLINEAR FE ANLAYSES

Jiangpeng Shu[1], Mario Plos[1], Kamyab Zandi[1,2], Morgan Johansson[1,3], Filip Nilenius[1]

[1]*Department of Civil and Environmental Engineering, Chalmers University of Technology, 412 96 Gothenburg, Sweden*
[2]*Concrete and Stone Group, CBI Swedish Cement and Concrete Research Institute, 501 15 Borås, Sweden*
[3]*Reinertsen Sweden AB, Kilsgatan 4, 411 04 Göteborg*

ABSTRACT

Reinforced concrete two-way slabs without shear reinforcement are commonly used in many structural systems. The paper investigated the structural behavior of RC slabs subjected to punching failure using solid nonlinear FE analysis. The appropriate approach to model the support was investigated and the non-tension spring was selected in the FE analysis. Nominal shear force distribution was studied for four type of slabs with different geometry of support, geometry of slab and layout of reinforcement. All the factors has been proved to influence the shear force distribution along control perimeter around the support. A new method based on shear field theory to calculate the effective control perimeter was validated in the study.

Keywords: shear distribution, RC slabs, punching shear, nonlinear FE analysis, control perimeter.

1. Introduction

Reinforced concrete two-way slabs without shear reinforcement are commonly used in many structural systems, such as bridge deck slabs, flat slabs of buildings, parking garages. Punching shear is usually the governing failure mode at ultimate of those RC slabs subjected to concentrated load. Currently, building codes such as ACI 318-05 (ACI Committee 318 2011) and EC2 2004 (EN 1992-1-1 2004) of practice provide several approaches to check the two-way punching strength of flat slabs. Such approaches typically propose a similar format, where the design shear strength (V_R) is estimated by multiplying a shear strength per unit length (nominal shear strength, v_R) by a control perimeter (b_0):

$$V_R = v_R \times b_0 \qquad \text{Equation 1}$$

The assumption is that the nominal shear force along the control perimeter is uniform. However, researchers has revealed that distribution of shear forces along the control perimeters is clearly uneven, and is influenced by several factors, such as geometry of the column (Vaz Rodrigues et al. 2008)(Sagaseta et al. 2014). With the help of shear field analysis, conclusion was drawn that shear failure surfaces developed in regions with the largest magnitude of shear force. Thus a new method to calculate the effective control perimeter was developed by Vaz Rodrigues and adopted by MC2010:

$$b_0 = \frac{V}{v_{\max}} \qquad \text{Equation 2}$$

This method has been validated by Vaz Rodrigues and Sagaseta and the nominal shear force distribution was obtained using linear FE analysis. However, how the nominal shear force distributed has not been investigated. In Plos *et al.,* [2], case studies have shown that more advanced methods normally yield an improved understanding of the structural response.

Therefore, the aim of this study is to investigate the shear force distribution of along control perimeter near a column or concentrated load. In order to reflect the influence of shear crack, a nonlinear FE analysis using continuum element was adopted in this study. Furthermore, the influence factors in two-way behavior, such as layout of reinforcement and geometry of column was investigated.

2. Modelling of RC slabs

2.1 Experimental slabs

The experimental sabs were test at École Polytechnique Fédérale de Lausanne (EPFL) from 2004 to 2015 by Muttoni *et al* (Guandalini et al. 2009), (Sagaseta et al. 2014), (Sagaseta et al. 2011) and (Einpaul et al. 2016). Four slabs (PG1, PT32, PE7 and AM 04) were selected for this study; see Figure 1 and Table 1. Square slab with square column PG1 was selected as a reference slab and other three were selected as comparative slabs. Compare to PG1, PT32 was selected because it changes layout of reinforcement; PE7 was selected since the geometry of slab was changed to octagon and shape of column was changed to circle; AM04 was selected because the geometry of column was changed to rectangular with ratio 1:3. These tested slabs were selected because the variation of these factors to shear force distribution would be investigated.

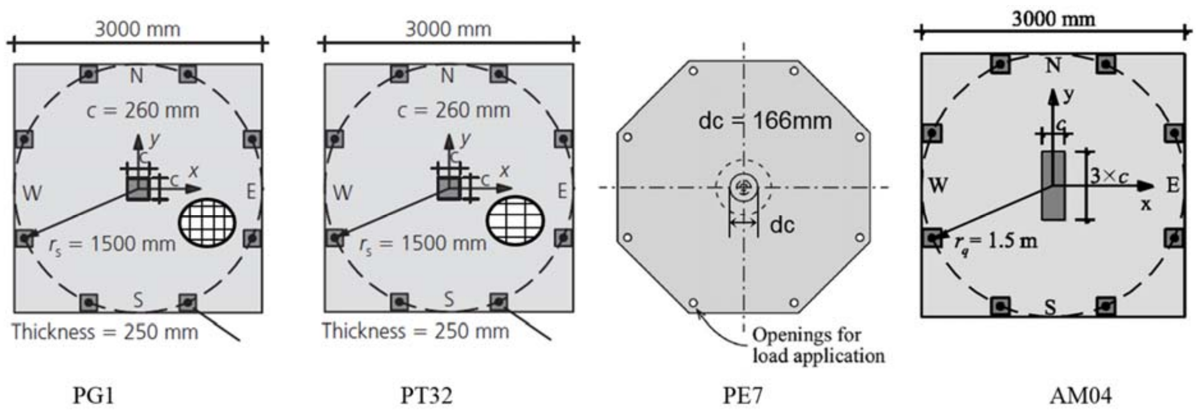

Figure 1: Experimental slabs

Table 1: Dimensions, reinforcement amounts and material properties of test series, from Guandalini & Muttoni (Guandalini et al. 2009).

Specimen dimension [m]		Concrete		Reinforcing steel		
		d [m]	f_c [MPa]	Reinforcement layout	ρ_x / ρ_y [%]	f_{yx} / f_{yy} [MPa]
B = 3.0 h = 0.25 c = 0.26	PG1	0.210	27.6	Ø20/20 s100	1.50% / 1.50%	542 / 542
	PT32	0.215	40	Ø20/16 s150	1.46% / 0.75%	540 / 558
	AM04	0.202	44.6	Ø16/16 s125	0.75% / 0.75%	516 / 516
B = 3.0 h = 0.25 d_c = 0.166	PE7	0.213	42.5	Ø20/20 s100	1.47% / 1.47%	542 / 542

2.2 Finite element model

The finite element software DIANA 9.5 (TNO 2014) was utilized to model the slabs, using 3D tetrahedron 4-node element models, as displayed in Figure 2. Due to symmetry and the need to reduce the computation time, only a quarter of the slab was included in the FE model. On the symmetry faces, all displacements perpendicular to the cross-sections were fixed. The reinforcement was modelled as fully bonded reinforcement bar. The loading steel plates above the slab were included and vertical displacement was fixed for the loading plates. Interface elements including Mohr-Coulomb friction model were used between the concrete and steel plates. To model the loading, all the nodes on the bottom surface of the column were tied to the centre node so that they had the same vertical displacement; during the analysis the centre node was given a controlled displacement upwards. An incremental, iterative static analysis was performed using specified increment sizes. Each increment was equivalent to a vertical displacement of 0.1 mm until the first crack initiated. After that, to save computation time, the increments were increased to 0.5 mm to save computation time. The analyses were carried out using a regular Newton-Raphson iteration method based on force and energy convergence criteria with a tolerance of 0.01. The FE model described above were applied to all the tested slabs.

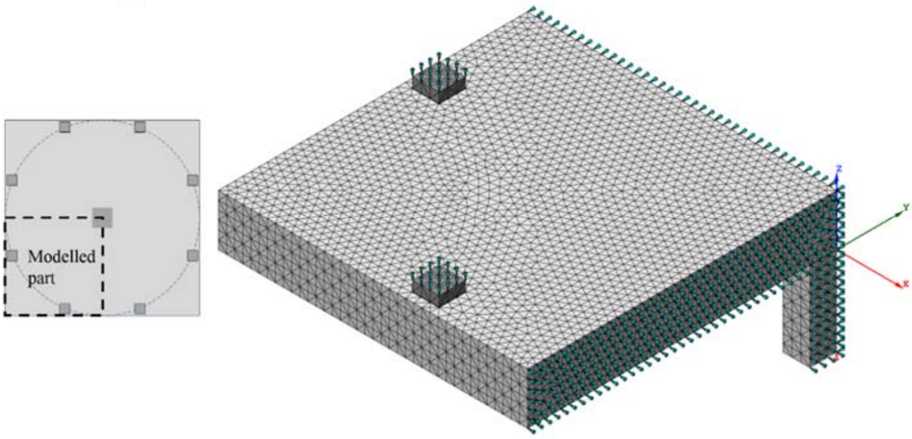

Figure 2: FE model of a quarter of slab PG1. Boundary conditions are indicated by arrows in the directions with fixed degrees of freedom.

2.3 *Modelling of support*

Before proceeding of FE analysis to all the tested slabs, the approach to model the support was investigated. Three different approach to model the support for PG1 was tested (see): (i) to use continuum element to model column directly; (ii) to use non-tension spring element to model column; (iii) to add pressure to the support area directly.

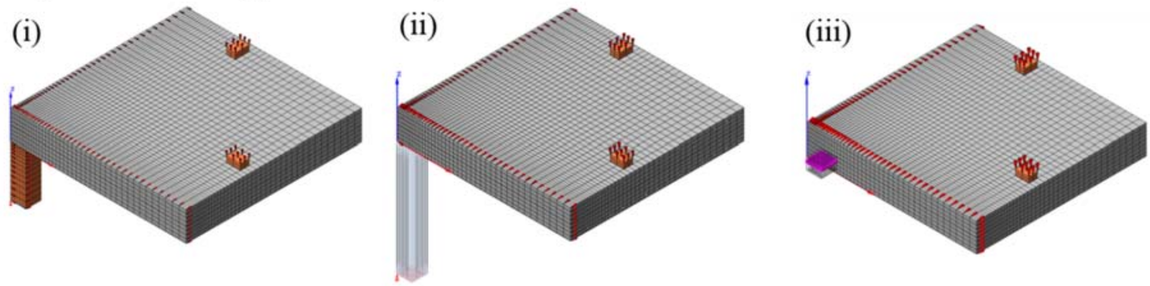

Figure 3: Three different alternative to model the support of PG1

The results show that to use non-tension spring element to model support yields similar results as to use continuum element to model support and they are close to the experiment. However, to add pressure to the support area directly underestimated the stiffness of the slab and load carrying capacity; see Figure 4. In addition, by observation of crack pattern in Figure 5, to add pressure to the support area also yielded different failure model compare to experiment. Thus the way to model support using spring was adopted in the continuing study.

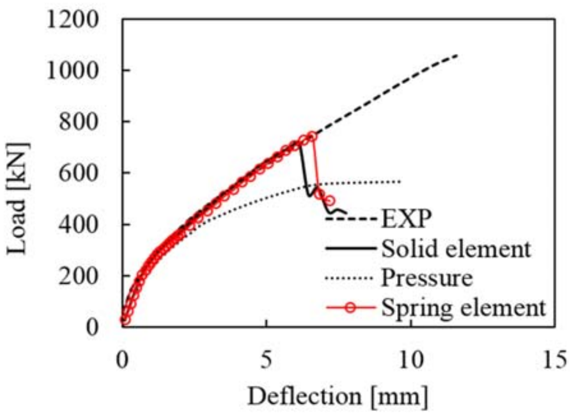

Figure 4: Load-deflection relation of PG1, using three different approach to model support

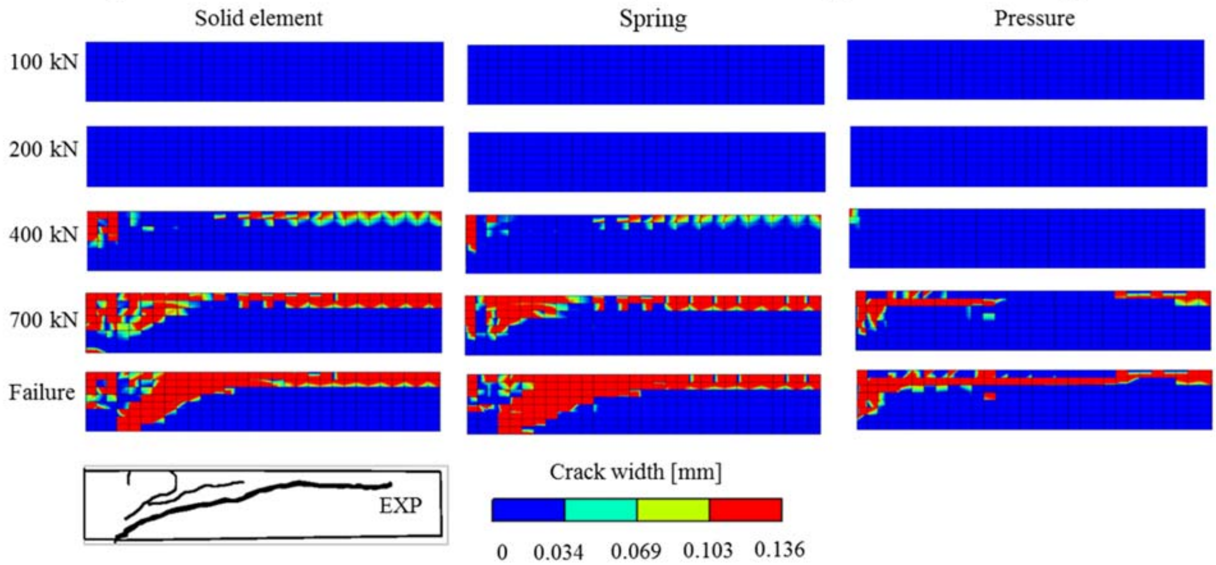

Figure 5: Crack pattern of PG1, using three different approach to model support

3. Results

3.1 Global structural behaviour

The load-rotation relation and crack pattern obtained from nonlinear FE analysis and the comparison to experiment are shown in Figure 6 and Figure 7. Figure 6 shows that the stiffness of RC slabs were reflected in the model accurately but the load-carrying capacity were underestimated sometimes. Figure 7 shows the crack patterns were predicted by the FE model with high accuracy.

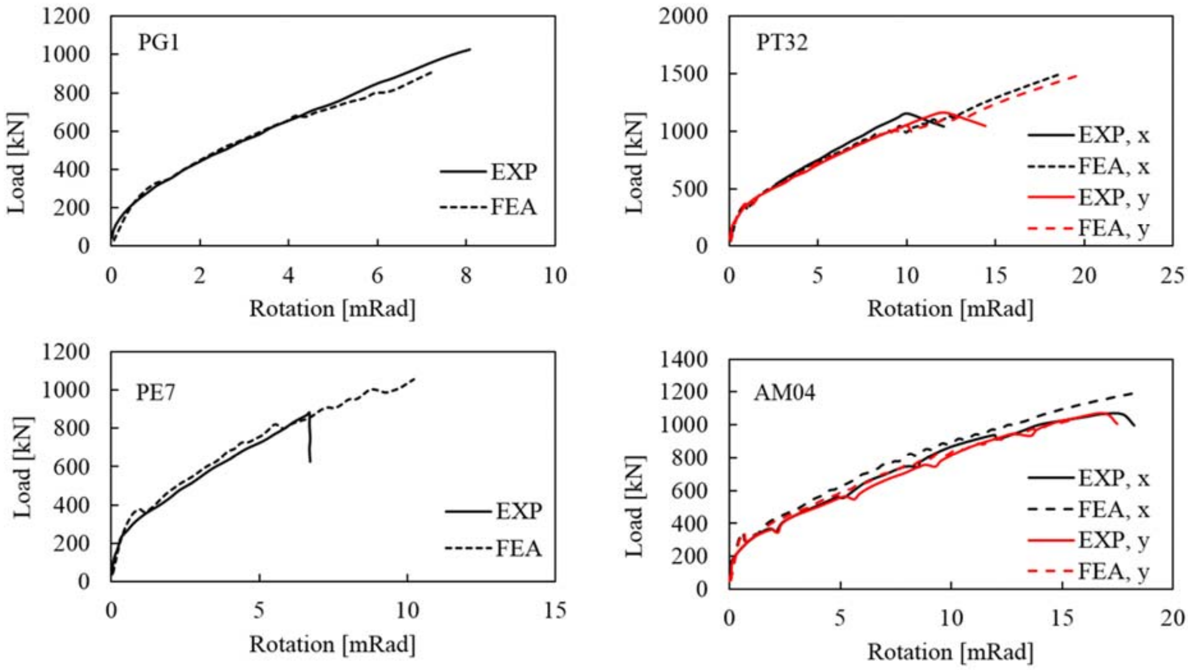

Figure 6: The load-rotation relation obtained from nonlinear FE analysis and the comparison to experiment.

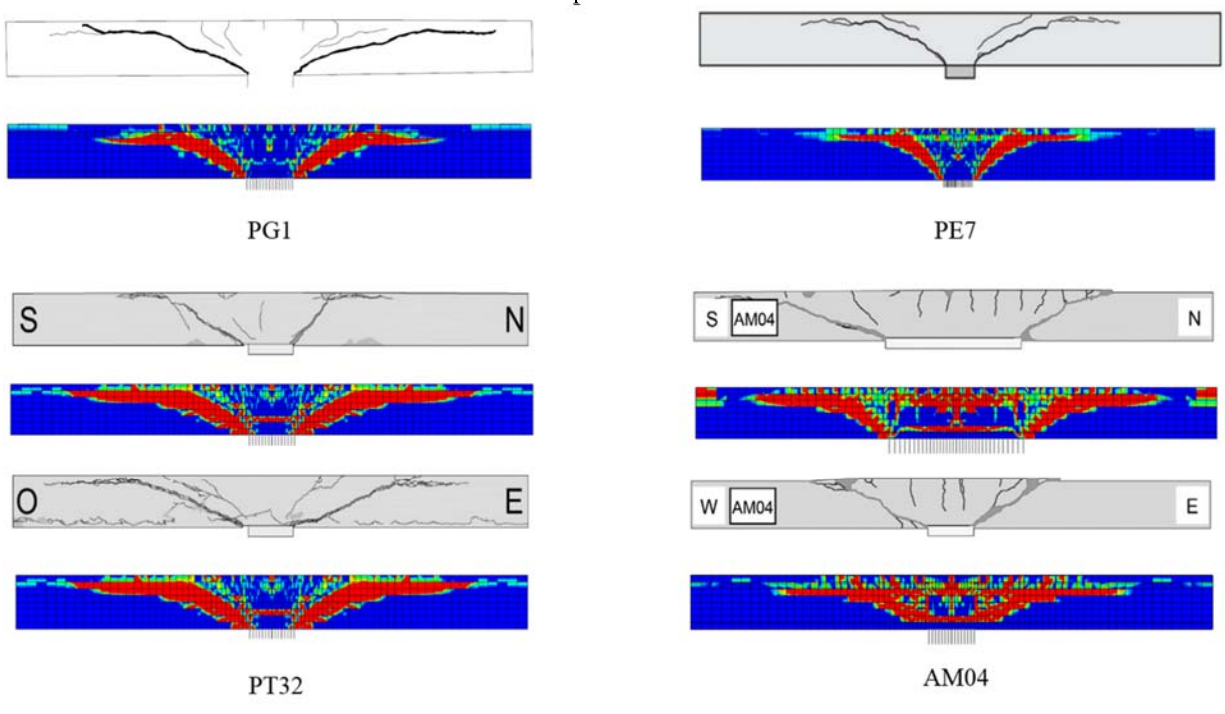

Figure 7: The crack pattern obtained from nonlinear FE analysis and the comparison to experiment.

3.2 Shear force distribution

The shear force distribution was investigated in the study; see Figure 8. Results shows that all the factors, geometry of slab, geometry of column and layout of reinforcement have impact to the shear force distribution. Furthermore, when the ratio between short side and long side for a rectangular column is larger than 3, the shear force distribution was influenced considerably due to stress concentration near the corner of the support.

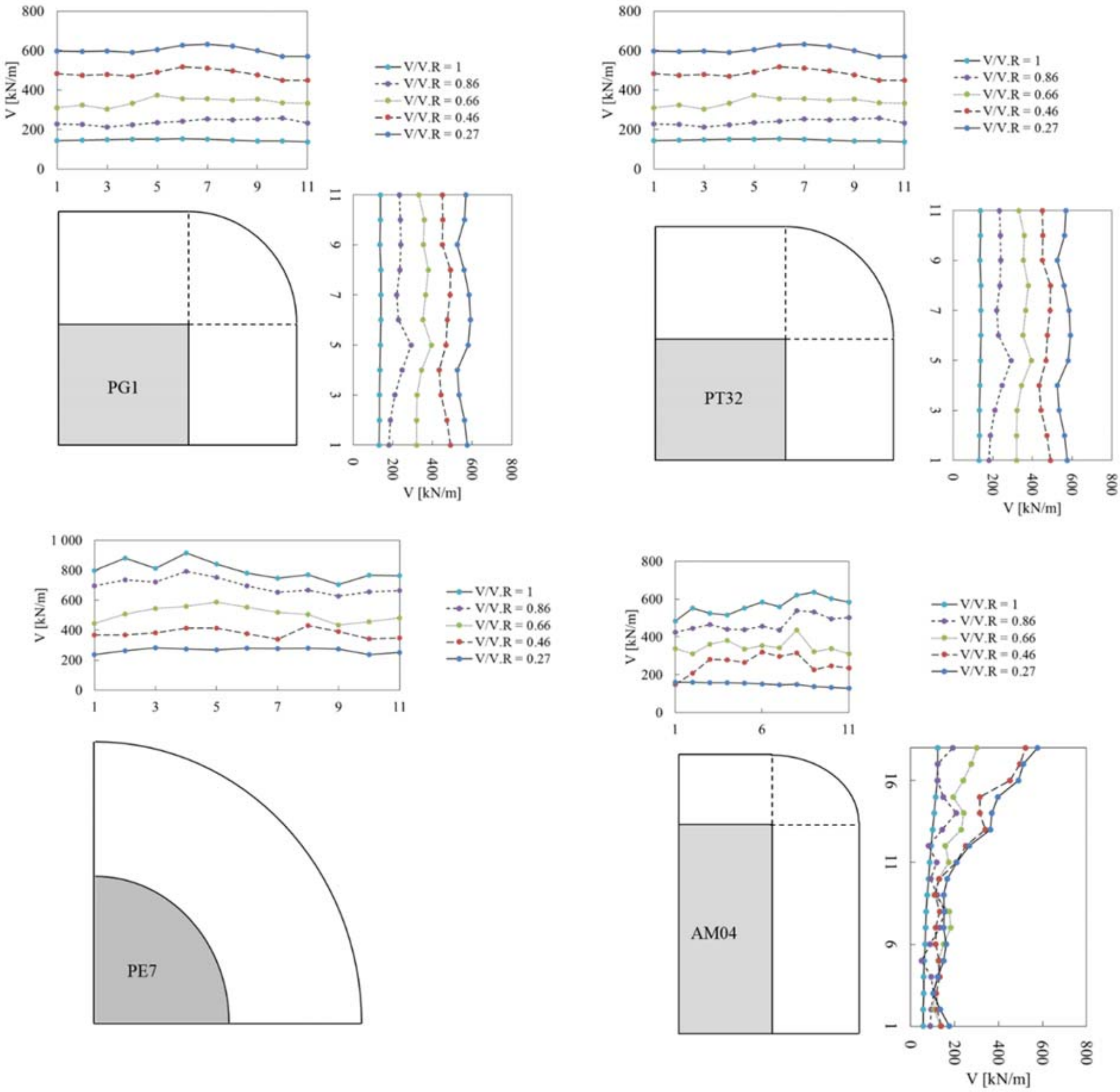

Figure 8: Nominal shear force distribution obtained from nonlinear FE analysis

3.3 Effective control perimeter

The effective control perimeter was calculated for all the four slabs according to Equation 2 and the results was presented in Table 2. b_0 is the effective control perimeter and b_1 is the standard value according to MC2010. The reduction factor α was also calculated for all the slabs and results is displayed in Figure 9. Results show that the reduction factor obtained in the cracked stage is lower than elastic stage. In addition, the slab with rectangular column (1:3) has much lower reduction factor than other slabs.

Table 2: The effective control perimeter and comparison to basic control perimeter

	PG1 b_1 = 1.669 m		PT32 b_1 = 1.715 m		PE7 b_1 = 1.190 m		AM04 b_1 = 2.714 m	
Load level [V/V_R]	b_0 [m]	b_0/b_1	b_0 [m]	b_0/b_1	b_0 [m]	b_0/b_1	b_0 [m]	b_0/b_1
0.27	1.48	0.89	1.50	0.87	1.07	0.90	1.81	0.67
0.46	1.32	0.79	1.50	0.88	1.00	0.84	1.45	0.53

0.66	1.42	0.85	1.39	0.81	1.02	0.86	1.51	0.55
0.86	1.44	0.86	1.39	0.81	1.03	0.87	1.61	0.59
1.00	1.44	0.86	1.43	0.83	1.01	0.85	1.57	0.58

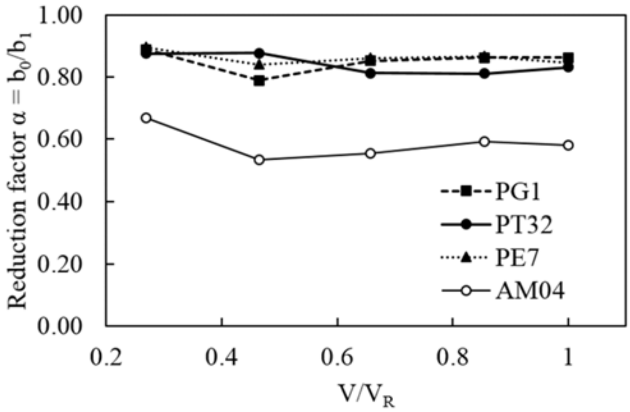

Figure 9: Reduction factor due to load level for different slabs

4. Conclusions

By the research above, such conclusions regarding structural behavior of RC slabs subjected to punching failure can be obtained.

- 3D nonlinear FE analysis are able to reflect the shear distribution for RC slabs subjected to punching.
- Shear distribution will be influence by geometry of slab and column.
- The updated effective control perimeter decreases when the applied load increase.

5. Acknowledgements

The authors would like to gratefully acknowledge the support and funding from Swedish Transport Administration (Trafikverket), which made the research possible. The study was also collaborated with École Polytechnique Fédérale de Lausanne (EPFL) in Switzerland and University of Parma in Italy.

References

ACI Committee 318, 2011. *Building Code Requirements for Structural Concrete and Commentary*, Farmington Hills, Mich: ACI American Concrete Institute.

Einpaul, J. et al., 2016. Study on Influence of Column Size and Slab Slenderness on Punching Strength. *ACI Structural Journal*, (113), pp.135–146.

EN 1992-1-1, 2004. *Eurocode 2: Design of concrete structures - part 1-1: General rules and rules for buildings.*, Brussels, Belgium: CEN European Committee for Standardization.

Guandalini, S., Burdet, O.L. & Muttoni, A., 2009. Punching tests of slabs with low reinforcement ratios. *ACI Structural Journal*, pp.87–95.

Sagaseta, J. et al., 2011. Non-axis-symmetrical punching shear around internal columns of RC slabs without transverse reinforcement. *Magazine of Concrete Research*, 63(6), pp.441–457. Available at: http://www.icevirtuallibrary.com/content/article/10.1680/macr.10.00098.

Sagaseta, J. et al., 2014. Punching of flat slabs supported on rectangular columns. *Engineering Structures*, 77, pp.17–33. Available at: http://dx.doi.org/10.1016/j.engstruct.2014.07.007.

TNO, 2014. *Diana finite element analysis, User's Manual -- Release 9.5*, TNO DIANA BV.

Vaz Rodrigues, R., Fernández Ruiz, M. & Muttoni, A., 2008. Shear strength of R/C bridge cantilever slabs. *Engineering Structures*, 30(11), pp.3024–3033.